[CTi$_7^{2+}$]: Heptacoordinate Carbon Motif?

Yi Gao,*,[†,‡] Nan Shao,[§] Rulong Zhou,[⊥] Guiling Zhang,[#] and Xiao Cheng Zeng*,[‡]

[†]Laboratory of Physical Biology and Division of Interfacial Water, Shanghai Institute of Applied Physics, Chinese Academy of Sciences, Shanghai 201800, China

[‡]Department of Chemistry, University of Nebraska—Lincoln, Lincoln, Nebraska 68588, United States

[§]Brookhaven National Laboratory, Upton, New York 11973, United States

[⊥]School of Science and Engineering of Materials, Hefei University of Technology, Hefei, Anhui, China 230009

[#]College of Chemical and Environmental Engineering, Harbin University of Science and Technology, Harbin, China 150080

Ⓢ Supporting Information

ABSTRACT: A heptacoordinate carbon motif $[CTi_7^{2+}]$ is predicted to be a highly stable structure (with D_{5h} point group symmetry) based on ab initio computation. This motif possesses a sizable HOMO−LUMO gap along with the lowest vibrational frequency greater than 95 cm^{-1}. An investigation of the motif-containing neutral species $[CTi_7^{2+}][BH_4^-]_2$ further confirms the chemical stability of the heptacoordinate carbon motif. In view of its structural stability, a quasi-one-dimensional (quasi-1D) nanowire $[CTi_7]_n[C_{16}H_8]_n$ is built from the carbon motifs. This organometallic nanowire is predicted to be metallic based on density functional theory computation.

Seven-Coordinated Carbon
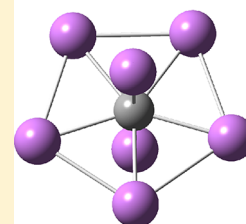
SECTION: Molecular Structure, Quantum Chemistry, and General Theory

Hypercoordinate carbon has long been a topic of interest to chemists. The first pentacoordinate carbon species CH$_5^+$ was isolated in 1952,[1] which is known to possess a highly fluxional three-dimensional (3D) structure. Thereafter, a large number of 3D hypercoordinate carbon species were synthesized in the laboratory.[2] On the other hand, the notion of planar tetracoordinate carbon (ptC) was proposed by Hoffmann and co-workers in 1970.[3,4] Shortly after, 1,1-dilithiocyclopropane was predicted to possess the ptC geometry based on ab initio calculation.[5] In 1977, the first experimental evidence of the ptC species was revealed by Cotton and Millar.[6] According to the valence shell electron pair repulsion (VSEPR) theory,[7] the valence electron pairs of carbon tend to repel each other to minimize their mutual repulsion. Hence, in most molecules, planar hypercoordinate carbon is energetically unfavorable. Nevertheless, the first planar tetracoordinate carbon species was initially predicted by Schleyer and Boldyrev in 1991[8] and later detected in experiments.[9,10] In 2000 and 2001, numerous planar pentacoordinate carbon (ppC) and planar hexacoordinate carbon (phC) species were predicted theoretically. For example, Exner and Schleyer showed that dianion CB$_6^{2-}$ and its isoelectronic species C$_3$B$_4$, both with six π electrons, were phC species.[11] Minyaev and Gribanova proposed heteroatomic extensions of CB$_6^{2-}$ to construct eight-membered ring perimeters.[12] The stability of this extended planar structure was confirmed recently by theoretical calculation.[13] Wang and Schleyer proposed a family of hyparenes, some of them incorporating a ppC motif within three borocarbon units.[14] A recent study by Wang, Boldyrev, and co-workers indicated that the most stable form of CB$_6^{2-}$ prefers a planar structure with a bicoordinate carbon atom.[15] Li et al. suggested a hydrocopper complex with a ppC motif.[16] Pei et al. reported the first theoretical evidence of a global-minimum ppC species, CAl$_5^+$.[17] Zhang et al. suggested four different types of compounds, all containing a ptC unit.[18] Wu et al. predicted the formation of a ptC stripe at the edge of a graphene nanoribbon decorated by certain metals.[19,20] To our knowledge, among all hypercoordinate carbon species reported in the literature, the highest coordinate number for the central carbon is six, and five is the maximum coordinate number for the most stable carbon species.[24] It is worth noting that the highest coordination number in a planar cluster species can be as high as 10 in metal-centered boron clusters.[21−24]

Herein, we show ab initio computational evidence of the possible existence of a highly stable heptacoordinate carbon motif, $[CTi_7^{2+}]$. Furthermore, we show that this motif can stably exist in the molecule $[CTi_7^{2+}][BH_4^-]_2$, whose structure is predicted to be stable at room temperature.[25]

The basin-hopping global optimization method coupled with density functional theory (DFT) optimization was employed to search for low-energy isomers of $[CTi_7^{2+}]$.[26,27] Two low-lying isomers, **1** and **2** (see Figure 1), are found, where **1** is a pentagonal bipyramid with D_{5h} point group symmetry. Other isomers are significantly higher in energy. The relative stability between the two low-energy isomers is examined using five different density functional methods for consistent evaluation, which include PBE,[28,29] ωB97xD,[30] B3LYP,[31,32] M06,[33] and
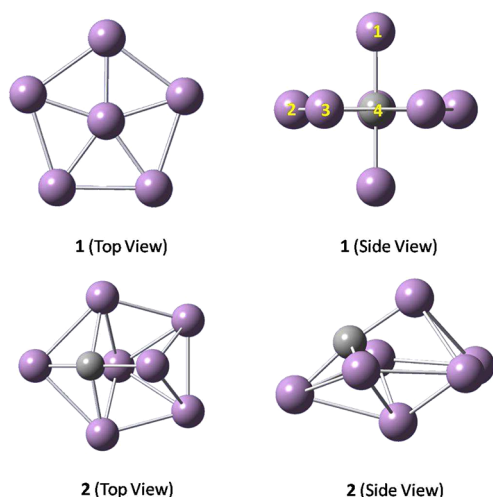
Figure 1. Optimized structures of hypercoordinate carbon isomer **1** and isomer **2** of $[CTi_7^{2+}]$. Gray spheres represent carbon atoms, and purple spheres represent titanium atoms.

TPSSh[34] functionals, all with the SDD[35,36] (for Ti) and 6-311+G(d) (for C) basis sets. The calculated energy differences are shown in Table 1. Clearly, all DFT methods suggest that **1**

Table 1. Energy Differences between Isomers 1 and 2 (eV), Where the Basis Sets Are SDD for Ti and 6-311+G(d) for C

	PBE	ωB97xD	B3LYP	M06	TPSSh
1	0.00	0.00	0.00	0.00	0.00
2	0.34	0.65	0.19	0.79	0.36

is 0.19−0.79 eV lower in energy than **2**. Harmonic vibrational frequencies are calculated at the same level of theory for the geometric optimization. No imaginary frequencies are found, suggesting that both isomers are local minima. For **1**, the lowest vibrational frequency is 131.8 cm^{-1} at the PBE level and 96.4 cm^{-1} at the B3LYP level, which are sufficiently large to meet a stability criterion suggested by Hoffmann et al.[25]

In isomer **1**, the central carbon atom is bonded with seven Ti atoms. Among the seven, five Ti atoms and the central C atom are in the same plane, forming a ppC motif, while the other two Ti atoms are located in the axial direction normal to the ppC plane. On the basis of structural optimization at the PBE level (little change is observed among optimized geometries using different DFT methods; see Table 2), the bond length between Ti and C in the ppC plane is 2.11 Å, nearly the same as the sum of covalent radii (Ti: 1.36 Å; C: 0.75 Å).[37] This bond length is slightly longer than the longest Ti−C bond length (2.09 Å) observed in the "met-car" cluster,[38,39] Ti$_8$C$_{12}$, and much shorter than the Ti−C bond length in the (η^5-C$_5$H$_5$)Ti[S$_2$CN(CH$_3$)$_2$]$_3$ sandwich nanowire.[40] The Ti−C bond length in the axial direction is 1.88 Å, between that of the single bond Ti−C and double bond Ti=C but shorter than the shortest bond (1.97 Å) in the cluster Ti$_8$C$_{12}$. The calculated Wiberg bond index (WBI)[41] for the five in-plane Ti−C bonds and two out-of-plane Ti−C bonds is 0.482 and 0.768, respectively. The Ti−Ti bond length between an out-of-plane Ti atom (Ti(**1**)) and in-plane Ti atoms (Ti(**2**)) is 2.83 Å, very close to the Ti−Ti bond length in Ti$_8$C$_{12}$ (2.81 Å).[38,39] The corresponding WBI for the Ti−Ti bond is 0.725. The Ti−Ti bond length in the ppC plane is 2.48 Å, and the corresponding WBI is 1.144.

Table 2. Optimized Geometry of $[CTi_7^{2+}]$ Isomer 1, HOMO and LUMO Energies, and Harmonic Vibrational Frequencies, Based on PBE and B3LYP Levels of Theory, and SDD (for Ti) and 6-311+G(d) (for C) Basis Sets

	PBE	B3LYP
Bond Length (Å)		
Ti(1)−Ti(2)	2.83	2.82
Ti(2)−Ti(3)	2.48	2.48
Ti(1)−C(4)	1.88	1.87
Ti(2)−C(4)	2.11	2.11
HOMO (eV)	−10.70	−9.96
LUMO (eV)	−11.50	−11.87
Harmonic Vib. (cm^{-1})		
lowest	131.8	96.4
highest	878.6	866.8

The isomer **1** of $[CTi_7^{2+}]$ has a relatively large energy gap between the highest occupied molecular orbital (HOMO) and lowest unoccupied molecular orbital (LUMO), about 0.80 eV at the PBE level and ~1.91 eV at the B3LYP level. The HOMO−LUMO gap is less than that of the global-minimum ppC species CAl$_5^+$. Both the HOMO and LUMO of the D_{5h}-$[CTi_7^{2+}]$ species are doubly degenerate. As shown in Figure 2,
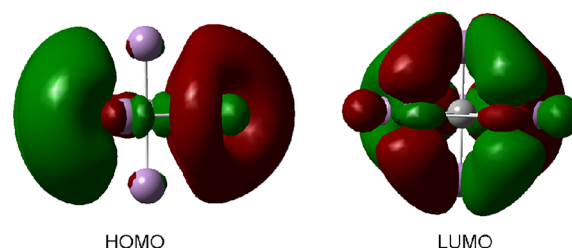

HOMO   LUMO

Figure 2. HOMO and LUMO of the CTi$_7^{2+}$ motif.

the HOMO is mostly contributed to by the 4s and 5s orbitals of the in-plane Ti$_5$ pentagon, while the LUMO is contributed to by both the 4s and 5s orbitals of five Ti atoms in the ppC plane and the 3d orbital of two Ti atoms in the axial direction. Considering that the C atom has four valence electrons and each Ti atom donates four valence electrons, $[CTi_7^{2+}]$ has 4(C) + 4 × 7(Ti) − 2 = 30 valence electrons. Applying Wade's 4n rule[42] to isomer **1** gives 30 valence electrons = 4 × 7 (number of vertices) + 2, suggesting that this cluster motif tends to adopt the pentagonal bipyramidal structure, consistent with our prediction. Wade's rule also provides an explanation for the high stability of isomer **1**.

To examine the chemical stability of the $[CTi_7^{2+}]$ cation motif in a molecular species, two $[BH_4]^-$ anions are attached to this motif to counterbalance the positive charge. A basin-hopping global-minimum search was performed on this molecular species. After further geometrical optimization, four low-lying isomers are identified, as shown in Figure 3, whose energy differences are within 1.0 eV (calculated at the PBE/SDD+6-311+G(d) level). Subsequent single-point energy computation performed at the coupled cluster (CCSD)[43] level [CCSD(T) calculation is computationally too demanding for our computer facility] confirms that the D_{5h}-$[CTi_7]^{2+}[BH_4^-]_2$ species with the heptacoordinate carbon is appreciably lower in energy than other three isomers. For example, the second-lowest isomer is 0.44 eV higher in CCSD
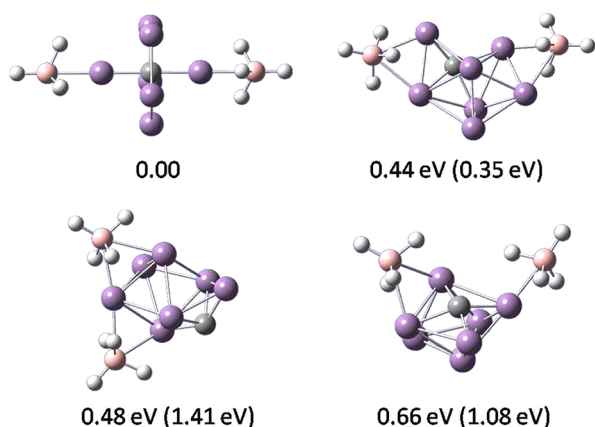
Figure 3. Four low-lying isomers of $[CTi_7^{2+}][BH_4^-]_2$ species. The energy differences are computed at the CCSD/SDD/6-311+G(d) level (PBE results are in parentheses). Gray spheres represent carbon atoms, purple spheres represent titanium atoms, pink spheres represent boron atoms, and white spheres represent hydrogen atoms.

energy. All of the calculations are performed with the Guassian09 software package.[44]

Further structural analysis shows that the CTi_7 motif maintains its structural integrity in the molecular species. The Ti–C bond lengths in the planar ring are 2.07 Å, slightly shorter than that in the pure motif, and the Ti–C bond in the axis is 1.97 Å, slightly longer than that in the pure motif. These bond lengths are closest to those in Ti_8C_{12} proposed by Pauling.[38] Six vibrational frequencies of the molecular species are less than 100 cm^{-1}, with the lowest frequency being 42 cm^{-1}. Nevertheless, all six low frequencies correspond to the vibrational modes associated with the BH_4 motif rather than with the CTi_7 motif, suggesting again that the $[CTi_7^{2+}]$ is indeed a highly stable motif and may be adopted as a building unit in other molecule species or nanostructures.

As an example, we use the $[CTi_7^{2+}]$ motif to construct a quasi-1D nanowire. Figure 4a and b displays two side views of a

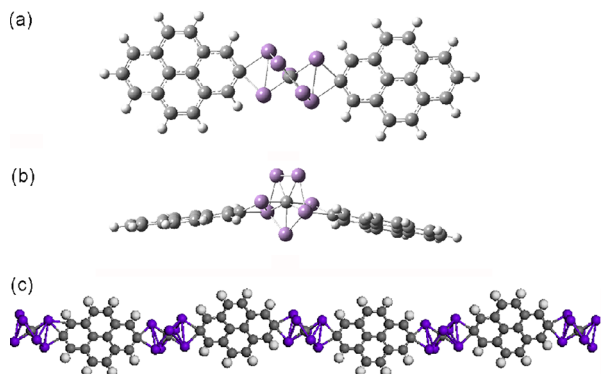**Figure 4.** (a) Top view of $[CTi_7][C_{16}H_9]_2$. (b) Side view of $[CTi_7][C_{16}H_9]_2$. (c) Nanowire structure of $[CTi_7]_n[C_{16}H_8]_n$.

$[CTi_7][C_{16}H_9]_2$ complex, which is composed of a $[CTi_7^{2+}]$ motif and two pyrene groups. The Ti–C bonds in the $[CTi_7^{2+}]$ are 2.08 and 1.94 Å, respectively, and the Ti–Ti bonds are 2.50, 2.68, and 2.81 Å, very close to those in the free $[CTi_7^{2+}]$ motif. The vibrational frequency calculation shows no imaginary frequencies, confirming the local stability of the complex. Using $[CTi_7][C_{16}H_8]$ as a structural unit, a quasi-1D nanowire $[CTi_7]_n[C_{16}H_8]_n$ can be constructed, as shown in Figure 4c.

The computed electronic density of states (DOS) is plotted in Figure 5, where it shows that the quasi-1D sandwich nanowire
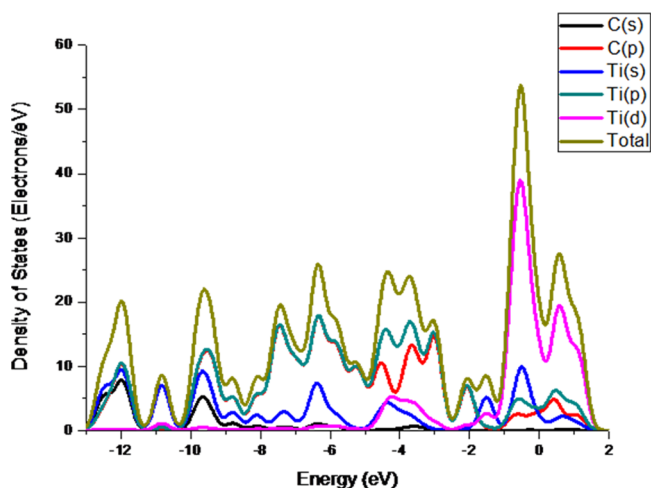

Figure 5. Electronic density of states (DOS) of quasi-1D $[CTi_7]_n[C_{16}H_8]_n$.

is metallic. The DOS near the Fermi level is mostly contributed to by the d orbital of Ti atoms, consistent with the LUMO diagram of the cluster dication (Figure 2). To further confirm the stability of the nanowire, an ab initio molecular dynamics simulation of $[CTi_7]_2[C_{16}H_8]_3H_2$ species is undertaken, with the temperature of the system being controlled at 400 K.[45,46] Here, the two H atoms are used to passivate the two ends of the finite-sized nanowire. After a 5 ps simulation, little change in the geometry of the nanowire is seen, suggesting that this nanowire is likely very stable at the ambient condition. To our knowledge, the $[CTi_7]_n[C_{16}H_8]_n$ sandwich nanowire is the first quasi-1D nanostructure that consists of a ppC motif.

In conclusion, we predict a highly stable hypercoordinate carbon motif $[CTi_7^{2+}]$ with a heptacoordinate carbon. This motif possesses a sizable HOMO−LUMO gap along with the lowest vibrational frequency greater than 95 cm^{-1}. Chemical stability of the motif is confirmed by the investigation of a neutral species, $[CTi_7^{2+}][BH_4^-]_2$. In view of the high stability of this motif, a quasi-1D periodic nanowire is constructed. This organometallic nanowire is predicted to be metallic. Possible existence of the heptacoordinate carbon species must await future experimental confirmation.

■ COMPUTATIONAL DETAILS

We combined the basin-hopping global-minimum method and DFT[26,27] to search for the low-energy candidates of $[CTi_7^{2+}]$ and $[CTi_7]^{2+}[BH_4^-]_2$. The two low-lying isomers of $[CTi_7^{2+}]$ were further optimized and vibrational-frequency-analyzed using PBE,[28,29] ωB97xD,[30] B3LYP,[31,32] M06,[33] and TPSSh[34] functionals, all with the SDD[35,36] (for Ti) and 6-311+G(d) (for C) basis sets. Four low-lying isomers of $[CTi_7]^{2+}[BH_4^-]_2$ were also optimized and vibrational-frequency-analyzed using PBE/SDD/6-311+G(d) level of theory. Their single-point energies were evaluated by CCSD calculations.[43] These calculations were performed with the Gaussian 09 software package.[44]

To test stability of the $[CTi_7]_n[C_{16}H_8]_n$ nanowire, we first optimized the structure of the $[CTi_7][C_{16}H_9]_2$ cluster using the PBE/SDD/6-311+G(d) level of theory. Its vibrational frequencies were further evaluated using the same level of theory. We then built the nanowire using $[CTi_7]_2[C_{16}H_8]_2$ as

the unit cell based on the geometric parameters of optimized $[CTi_7][C_{16}H_9]_2$. The unit cell is 26.557 Å $\times$ 20 Å $\times$ 20 Å. The geometric optimization and DOS evaluations were further carried out at the Γ-point using the PBE/DNP level of theory and a semicore pseudopotential.[45,46] The orbital cutoff was set at 4.5 Å, and the threshold for SCF convergence was 10^{-5} Hartree. In addition, using $[CTi_7]_2[C_{16}H_8]_3H_2$ as an example of finite-sized nanowire, we performed an ab initio molecular dynamics simulation (at the level of PBE/DNP) for 5 ps to examine the thermal stability of the nanowire. The massive Nose−Hoover chain method was used to control the temperature of the system (maintained at 400 K). DFT calculations and ab initio molecular dynamics simulation were performed using the DMol^3 software package.[45,46]

■ ASSOCIATED CONTENT

Ⓢ Supporting Information

Complete ref 44 and coordination of the structures. This material is available free of charge via the Internet at http://pubs.acs.org.

■ AUTHOR INFORMATION

Corresponding Author

*E-mail: gaoyi@sinap.ac.cn (Y.G.); xzeng1@unl.edu (X.C.Z.).

Notes

The authors declare no competing financial interest.

■ ACKNOWLEDGMENTS

■ ABBREVIATIONS

3D, three-dimensional; ptC, planar tetracoordinate carbon; ppC, planar pentacoordinate carbon; phC, planar hexacoordinate carbon; PBE, Perdew−Burke−Ernzerhof functional; ωB97xD, Head-Gordon's latest functional with inclusion of empirical dispersion; B3LYP, Becke's three parameter hybrid functional with the Lee−Yang−Parr correlation functional; M06, hybrid meta-functional of Truhlar and Zhao; TPSSh, hybrid functional of Tao, Perdew, Staroverow, and Scuseria; CCSD, coupled cluster method including single and double substitution

■ REFERENCES

(1) Tal'roze, V. L.; Lyubimova, A. K. Secondary Processes in the Ion Source of a Mass Spectrometer. *Dokl. Bulg. Akad. Nauk. SSSR* **1952**, *86*, 909−912.

(2) Olah, G. A. et al. *Hydrocarbon Chemistry*; Wiley-Interscience: New York, 1987.

(3) Hoffmann, R.; Alder, R. W.; Wilcox, C. F., Jr. Planar Tetracoordinate Carbon. *J. Am. Chem. Soc.* **1970**, *92*, 4992−4993.

(4) Hoffmann, R. The Theoretical Design of Novel Stabilized Systems. *Pure Appl. Chem.* **1971**, *28*, 181−194.

(5) Collins, J. B.; Dill, J. D.; Jemmis, E. D.; Apeloig, Y.; Schleyer, P. v. R.; Seeger, R.; Pople, J. A. Stabilization of Planar Tetracoordinate Carbon. *J. Am. Chem. Soc.* **1976**, *85*, 5419−5427.

(6) Cotton, F. A.; Miller, M. J. The Probable Existence of a Triple Bond between Two Vanadium Atoms. *Am. Chem. Soc* **1977**, *99*, 7886−7891.

(7) Gillespie, R. J.; Popelier, L. A. *Chemical Bonding and Molecular Geometry: From Lewis to Electron Densities*; Oxford University Press: Oxford, 2011.

(8) Schleyer, P. v. R.; Boldyrev, A. I. A New General Strategy for Achieving Planar Tetracoordinate Geometries for Carbon and Other Second Row Periodic Elements. *J. Chem. Soc., Chem. Commun.* **1991**, 1536−1538.

(9) Li, X.; Wang, L. S.; Boldyrev, A. I.; Simons, J. Tetracoordinated Planar Carbon in the AlC$^-$ Anion: A Combined Photoelectron Spectroscopy and Ab Initio Study. *J. Am. Chem. Soc.* **1999**, *121*, 6033−6038.

(10) Wang, L. S.; Boldyrev, A. I.; Li, X.; Simons, J. Experimental Observation of Pentaatomic Tetracoordinate Planar Carbon-Containing Molecules. *J. Am. Chem. Soc.* **2000**, *122*, 7681−7687.

(11) Exner, K.; Schleyer, P. v. R. Planar Hexacoordinate Carbon: A Viable Possibility. *Science* **2000**, *290*, 1937−1940.

(12) (a) Minyaev, R. M.; Gribanova, T. N. Stabilization of Nonclassical Types of Valence Bond Orientation at the Carbon Atom in Organoboron Compounds. *Izv. Akad. Nauk. Ser. Khim.* **2000**, *5*, 786−796. (b) Minyaev, R. M.; Gribanova, T. N. *Russ. Chem. Bull.* **2000**, *49*, 783−793.

(13) Ito, K.; Chen, Z.; Cormingboeuf, C.; Wannere, C. S.; Zhang, X. H.; Li, Q. S.; Schleyer, P. v. R. Myraid Planar Hexacoordinate Carbon Molecules Inviting Synthesis. *J. Am. Chem. Soc.* **2007**, *129*, 1510−1511.

(14) Wang, Z.; Schleyer, P. v. R. Construction Principles "Hyparenes": Families of Molecules with Planar Pentacoordinate Carbons. *Science* **2001**, *292*, 2465−2469.

(15) Averkiev, B. B.; Zubarev, D. Y.; Wang, L.-M.; Huang, W.; Wang, L.-S.; Boldyrev, A. I. Carbon Avoids Hypercoordination in CB_6^-, CB_6^{2-}, and $C_2B_5^-$ Planar Carbon−Boron Clusters. *J. Am. Chem. Soc.* **2008**, *130*, 9248−9250.

(16) Li, S. D.; Miao, C. Q.; Guo, J. C.; Ren, G. M. D_{5h} Cu_5H_5X: Pentagonal Hydrocopper Cu_5H_5 Containing Pentacoordinate Planar Nonmetal Centers (X = B, C, N, O). *Eur. J. Inorg. Chem.* **2004**, *11*, 2232−2234.

(17) Pei, Y.; An, W.; Ito, K.; Schleyer, P. v. R.; Zeng, X. C. Planar Pentacoordinate Carbon in CAl_5^+: A Global Minimum. *J. Am. Chem. Soc.* **2008**, *130*, 10394−10400.

(18) Zhang, X.-M.; Lv, J.; Ji, F.; Wu, H.-S.; Jiao, H.; Schleyer, P. v. R. A Perfectly Square-Planar Tetracoordinated Oxygen in a Tetracopper Cluster-Based Coordination Polymer. *J. Am. Chem. Soc.* **2011**, *133*, 4788−4790.

(19) Wu, M. H.; Pei, Y.; Zeng, X. C. Planar Tetracoordinate Carbon Strips in Edge Decorated Graphene Nanoribbon. *J. Am. Chem. Soc.* **2010**, *132*, 5554−5555.

(20) Wu, M. H.; Pei, Y.; Dai, J.; Li, H.; Zeng, X. C. Tri-Wind Graphene Nano-Paddle-Wheel with a Single-File Metal Joint: Formation of Multi-Planar Tetracoordinated-Carbon (ptC) Strips. *J. Phys. Chem. C* **2012**, *116*, 11378−11385.

(21) Romanescu, C.; Galeev, T. R.; Li, W.-L.; Boldyrev, A. I.; Wang, L. S. Aromatic Metal-Centered Monocyclic Boron Rings: Co@B$_8^-$ and Ru@B$_9^-$. *Angew. Chem., Int. Ed.* **2011**, *50*, 9334−9337.

(22) Li, W.-L.; Romanescu, C.; Galeev, T. R.; Piazza, Z. A.; Boldyrev, A. I.; Wang, L. S. Transition-Metal-Centered Nine-Membered Boron Rings: M@B$_9$ and M@B$_9^-$ (M = Rh, Ir). *J. Am. Chem. Soc.* **2012**, *134*, 165−168.

(23) Galeev, T. R.; Rlomanescu, C.; Li, W.-L.; Wang, L. S.; Boldyrev, A. I. Observation of the Highest Coordniation Number in Planar Species: Decacoordinated Ta@B$_{10}^-$ and Nb@B$_{10}^-$ Anions. *Angew. Chem., Int. Ed.* **2012**, *51*, 2101−2105.

(24) Heine, T.; Merino, G. What Is the Maximum Coordination Number in a Planar Structure? *Angew. Chem., Int. Ed.* **2012**, *51*, 4275−4276.

2267

dx.doi.org/10.1021/jz300859t | J. Phys. Chem. Lett. 2012, 3, 2264−2268

(25) Hoffmann, R.; Schleyer, P. v. R.; Schaefer, H. F., III. Predicting Molecules—More Realism, Please! *Angew. Chem., Int. Ed.* **2008**, *47*, 7164−7167.

(26) Wales, D. J.; Scheraga, H. A. Global Optimization of Clusters, Crystals and Biomolecules. *Science* **1999**, *285*, 1368−1372.

(27) Bai, J.; Cui, L.-F.; Wang, J. L.; Yoo, S.; Li, X.; Jellinek, J.; Koehler, C.; Frauenheim, Th.; Wang, L. S.; Zeng, X. C. Structural Evolution of Anionic Silicon Clusters Si_N (20 < N < 45). *J. Phys. Chem. A* **2006**, *110*, 908−912.

(28) Perdew, J. P.; Burke, K.; Ernzehof, M. Generalized Gradient Approximation Made Simple. *Phys. Rev. Lett.* **1996**, *77*, 3865−3868.

(29) Perdew, J. P.; Burke, K.; Ernzerhof, M. Generalized Gradient Approximation Made Simple. *Phys. Rev. Lett.* **1997**, *78*, 1396.

(30) Chai, J.-D.; Head-Gordon, M. Large-Range Corrected Hybrid Density Functionals with Damped Atom-atom Dispersion Corrections. *Phys. Chem. Chem. Phys.* **2008**, *10*, 6615−6620.

(31) Becke, A. D. Density-Functional Exchange-Energy Approximation with Correct Asymptotic Behavior. *Phys. Rev. A* **1988**, *38*, 3098−3100.

(32) Lee, C.; Yang, W.; Parr, R. G. Development of the Colle-Salvetti Correlation-Energy Formula into a Functional of the Electron Density. *Phys. Rev. B* **1988**, *37*, 785−789.

(33) Zhao, Y.; Trular, D. G. The M06 Suite of Density Functionals for Main Group Theomochemistry, Theomochemical Kinetics, Noncovalent Interactions, Excited States, and Transition Elements: Two New Functionals and Systematic Testing of Four M06-Class Functionals and 12 Other Functionals. *Theor. Chem. Acc.* **2008**, *120*, 215−241.

(34) Tao, J. M.; Perdew, J. P.; Staroverov, V. N.; Scuseria, G. E. Climbing the Density Functional Ladder: Nonempirical Meta-Generalized Gradient Approximation Designed for Molecules and Solids. *Phys. Rev. Lett.* **2003**, *91*, 146401.

(35) Dolg, M.; Wedig, U.; Stoll, H.; Preuss, H. Energy-Ajusted ab initio Pseudopotentials for the First Row Transition Elements. *J. Chem. Phys.* **1987**, *86*, 866−872.

(36) Schwerdtfeger, P.; Dolg, M.; Schwarz, W. H. E.; Bowmaker, G. A.; Boyd, P. D. W. Relativistic Effects in Gold Chemistry. I. Diatomic Gold Compounds. *J. Chem. Phys.* **1989**, *91*, 1762−1774.

(37) The atom and ion size comes from *WebElements*. http://www.webelements.com/atom_sizes.html (2012).

(38) Pauling, L. Molecular Structure of Ti_8C_{12} and Related Complexes. *Proc. Natl. Acad. Sci. U.S.A.* **1992**, *89*, 8175−8176.

(39) Chen, H.; Feyereisen, M.; Long, X. P.; Fitzgerald, G. Stability, Bonding, and Geometric Structure of Ti_8C_{12}, Ti_8N_{12}, V_8C_{12}, and Zr_8C_{12}. *Phys. Rev. Lett.* **1993**, *71*, 1732−1735.

(40) Steffen, W. L.; Chun, H. K.; Fay, R. T. Crystal and Molecular Structure of .eta.5-cyclopentadienyltris(N,N-dimethyldithiocarbamato)titanium(IV), A Stereochemically Rigid Seven-Coordinate Chelate. *Inorg. Chem.* **1978**, *17*, 3498−3503.

(41) Martin, F.; Zipse, H. Charge Distribution in the Water Molecule—A Comparison of Methods. *J. Comput. Chem.* **2005**, *26*, 97−105.

(42) Mingos, D. M. P. Polyhedral Skeletal Electron Pair Approach. *Acc. Chem. Res.* **1984**, *17*, 311−319.

(43) Cizek, J. In *Advances in Chemical Physics*; Hariharan, P. C., Ed.; Wiley Interscience: New York, 1969, Vol. *14*.

(44) Frisch, M. J.; et al. *Gaussian 09*, revision A.01; Gaussian, Inc.: Wallingford, CT, 2009.

(45) Delley, B. J. An All-Electron Numerical Methodfor Solving the Local Density Functional for Polyatomic Molecules. *J. Chem. Phys.* **1990**, *92*, 508−517.

(46) Delley, B. From Molecules to Solids with the DMol[3] Approach. *J. Chem. Phys.* **2000**, *113*, 7756−7764.